Influence of the surface properties of nanocapsules on their interaction with intestinal barriers

Irene Santalices[a,b], Dolores Torres[b], Mª Victoria Lozano[c,d], Mª Mar Arroyo-Jiménez[c,d], María José Alonso[a,b*], Manuel J. Santander-Ortega[c,d]**

[a]Center for Research in Molecular Medicine and Chronic Diseases (CIMUS), Campus Vida, University of Santiago de Compostela, Santiago de Compostela 15782, Spain.
[b]Department of Pharmaceutics and Pharmaceutical Technology, School of Pharmacy, Campus Vida, University of Santiago de Compostela, Santiago de Compostela 15782, Spain.
[c]Cellular Neuroanatomy and Molecular Chemistry of Central Nervous System Group, School of Pharmacy, University of Castilla-La Mancha, Albacete 02071, Spain.
[d]Regional Centre of Biomedical Research (CRIB), University of Castilla-La Mancha, Albacete 02071, Spain.

[*]Corresponding author e-mail address: mariaj.alonso@usc.es

[**]Corresponding author e-mail address: manuel.santander@uclm.es

E-mail addresses: irene.santalices@hotmail.es (I. Santalices); dolores.torres@usc.es (D. Torres); mvictoria.lozano@uclm.es (M. V. Lozano); mariamar.arroyo@uclm.es (M. Arroyo-Jiménez); mariaj.alonso@usc.es (M. J. Alonso); manuel.santander@uclm.es (M.J. Santander-Ortega).

Abstract

Despite the convenience of the oral route for drug administration, the existence of different physiological barriers associated with the intestinal tract greatly lowers the bioavailability of many active compounds. We have previously suggested the potential polymeric nanocapsules, consisting of an oily core surrounded by a polymer shell, as oral drug delivery carriers. Here we present a systematic study of the influence of the surface properties of these nanocapsules on their interaction with the intestinal barriers. Two different surfactants, Pluronic®F68 (PF68) and F127 (PF127), and two polymeric shells, chitosan (CS) and polyarginine (PARG) were chosen for the formulation of the nanocapsules. We analyzed nine different combinations of these polymers and surfactants, and studied the effect of each specific combination on their colloidal stability, enzymatic degradation, and mucoadhesion/mucodiffusion. Our results indicate that both, the polymer shell and the surfactants located at the oil/water interface, influence the interaction of the nanocapsules with the intestinal barriers. More interestingly, according to our observations, the shell components of the nanosystems may have either synergic or disruptive effects on their capacity to overcome the intestinal barriers.

Keywords: poloxamer, chitosan, polyarginine, nanocarrier, nanocapsule, colloidal stability, lipolysis, mucoadhesion, mucodiffusion, oral administration

Abbreviations: chitosan (CS), nanocapsules (NCs), nanoemulsion (NE), poloxamer 188 (PF68), poloxamer 407 (PF127), polyarginine (PARG), polyethylene oxide (PEO), propylene oxide (PPO), simulated intestinal fluid (SIF).

1. Introduction

The oral route is one of the most accepted routes for the administration of drugs, especially in the case of chronic treatments. Despite having an adequate patient compliance, this route of administration has several well-known physiological barriers that hamper the administration of many drugs. When administrated orally, the drugs must overcome several hurdles, such as their potential degradation by the intestinal enzymes, their instability in the presence of high ionic forces at different pHs, and their difficulty to pass through the intestinal mucosa [1,2]. The existence of all these physiological barriers influences particularly the bioavailability of certain active substances (e.g. peptides and proteins) after oral administration and, hence, their potential therapeutic effect [3–6].

Some of the strategies proposed to improve the oral bioavailability of peptides and proteins refer to the incorporation into their formulation of absorption enhancers or enzyme inhibitors [7–14]. This variety of formulation strategies has opened new avenues for the increasing number of peptidic drugs in industry pipelines [15,16]. However, despite the improved bioavailability of some drugs when associated with nanocarriers [17], advances in this area have been hampered by the limited knowledge about the effect of the physicochemical properties and composition of the nanocarriers in their interaction with the intestinal tract [13,18].

The high concentration of electrolytes and enzymes in the intestinal environment is a major obstacle for the maintenance of the integrity of the nanocarriers and of their associated active compounds, since they can undergo degradation even before reaching the intestinal epithelium. In this scenario, the role of pancreatin, a combination of amylases, lipases and proteases enzymes, is particularly relevant [19–21]. Consequently, to understand the influence that the properties and composition of these nanocarriers have on their interaction with these enzymes is crucial to further advance in this field.

Additionally, the intestinal epithelium is covered by a mucus layer whose biological function is to keep the epithelium lubricated and protected from pathogens and exogenous substances [22]. The mucus layer, with a thickness that varies along the intestinal tract [23,24], consists of a first layer firmly attached to the cellular epithelium

and a second layer that is constantly being replaced [25–27]. This is why, mucoadhesive colloidal systems, specially designed to interact with the intestinal mucus [28–30], may become immobilized in the superficial mucus layer, and eventually removed [26,31,32]. Therefore, the nanocarriers intended for oral drug delivery must exhibit an adequate mucoadhesive/mucodiffusive balance.

Based on this information, the objective of this work was to evaluate the effect of the surface composition of different oily-based nanocarriers (nanoemulsions and nanocapsules) on their capacity to overcome specific barriers associated to the oral modality of administration. The basis for the selection of the nanocarriers relies of previous activity from our group showing the potential of chitosan (CS) nanocapsules (NCs) and polyarginine (PARG) NCs for the oral administration of salmon and insulin, respectively [33–39]. These nanocarriers are composed of an oily core and a polymeric shell, which is the main determinant for the interaction with the surrounding medium. Overall, the behaviour of nine nanosystems containing different surfactants and polymer shells was investigated (*Figure 1*). A nanoemulsion (NE) consisting of Miglyol®812N and Epikuron®145V lecithin was used as reference in order to study the effect of the Pluronic® surfactant F68 and F127 , as well as that of the cationic polymers CS and PARG. In total, 3 different NEs and 6 different NCs were systematically analyzed for their capacity to overcome specific intestinal barriers. Namely, we evaluated the nanosystems for *i)* their stability, both colloidal and chemical, in simulated intestinal fluid and *ii)* their interaction (adhesion and diffusion) with mucus, while mimicking the physiological conditions [27,40].

2. Materials and methods

2.1. Materials

For the preparation of nanosystems, the neutral oil Miglyol®812N, a triglyceride formed from medium-chain fatty acids (capric and caprilic acids) was kindly donated by Cremer Oleo Division (Germany); soybean lecithin (Epikuron®145V), used as surfactant in the oily phase, was supplied by Cargill (Spain); poloxamer 188 (Pluronic®F68–PF68) and poloxamer 407 (Pluronic®F127–PF127), used as surfactants in the aqueous phases, were supplied by Sigma-Aldrich (Spain). *Table 1* shows the chemical structure and main characteristics of both poloxamers. According to the HLB values, PF68 is more hydrophilic than PF127. The polysaccharide chitosan (deacetylation degree: 75−90 %; MW ≈ 113 KDa) and the polyamino acid poly-L−arginine (MW ≈ 5−15 KDa), selected as cationic polymers, were purchased from FMC Biopolymer (USA) under the commercial name of Protasan Cl 113 and Sigma-Aldrich (Spain) respectively. When necessary, the lipophilic tracer DiD (DiIC18(5) oil (1,1'−dioctadecyl-3,3,3',3'−tetramethylindodicarbocyanine

perchlorate)) used as fluorescent dye ($\lambda_{ex} \approx 644$ nm, $\lambda_{em} \approx 665$ nm) was supplied by Invitrogen (Belgium).

Table 1: Chemical structure and main characteristics of Pluronic®F68 and Pluronic®F127*. PEO: polyethylene oxide unit; PPO: propylene oxide unit. MW: molecular weight. HLB: hydrophilia-lipophilia balance.*
[Table 1]

For the stability studies, pancreatin from porcine pancreas (4 × USP) was supplied by Sigma-Aldrich (Spain). For the mucoadhesion studies, partially purify mucin type III from porcine stomach and poly-D−lysine hydrobromide were purchased from Sigma-Aldrich (Spain). Glass bottom dishes (35 mm dish with 14 mm glass diameter, uncoated) were purchased from MatTek Corporation (USA). For mucodiffusion studies square borosilicate capillaries (0.6 square ID (mm) × 0.12 wall (mm)) were purchased from VitroCom (USA).

2.2. Preparation of nanoemulsions and nanocapsules

For this study, nine different formulations were prepared (*Figure 1, lower panel*), according to the two-step procedure previously described by our group (*Figure 1, upper panel*) [41]. First, we prepared the primary NE by the solvent displacement technique [37–40,42]. Briefly, an organic phase consisting of 20 mg of lecithin dissolved at 37 °C in 0.25 mL of ethanol, 62.5 µL of Miglyol®812N, and acetone to a total volume of 5 mL, and then poured onto 10 mL of ultrapure water under constant magnetic stirring (500 rpm). The mixture turned milky immediately due to the formation of the NE. After stirring for 10 minutes, the solvents were evaporated under vacuum to a final volume of 4 mL. When necessary, in a second step, this primary NE was coated with the correspondent surfactants (PF68 and PF127) and polymers (CS and PARG) by simple incubation in the aqueous solutions of these components or simply diluted with ultrapure water to obtain the different NEs-surfactant and NCs [33,43] having always the same concentration of the common components present in the core. More specifically, 4 mL of the primary NE were incubated under magnetic stirring for 10 minutes with 1 mL of aqueous solution containing or not, the corresponding polymer (CS – 5 mg/mL or PARG – 2.5 mg/mL) or/and the surfactant (PF68 or PF127 – both of them 25 mg/mL), which led to the formation of the final nanosystems. Concentration of coating materials was chosen according to previously reported works [39,41,44].

When a fluorescent marker was needed, DiD was incorporated to the oily core by substitution of 80 µL of ethanol by the same volume of an ethanol DiD solution (2.5 mg/mL).

[Figure 1]

Figure 1. Schematic representation of the formulation procedure (upper panel) and the nanosystems tested (lower panel). *Laboratory material and equipment (https://creativecommons.org/licenses/by/3.0/) have been modified from the original work provided by Servier Medical Art (http://smart.servier.com/).*

2.3. Characterization of the physicochemical properties and DiD encapsulation efficiency of the nanosystems

Size and polydispersity index of the blank nanosystems were analyzed by photon correlation spectroscopy, and ζ−potential was determined by laser Doppler anemometry using a Malvern Zeta-sizer device (NanoZS, ZEN 3600, Malvern Instruments, Worcestershire, UK). To obtain DLS measurements, nanosystems were appropriately diluted (30 µL of nanosystems + 970 µL of dilution medium) in ultrapure water to determine their size, and in a low ionic strength saline medium to determine their ζ−potential ($n \geq 3$).

The encapsulation efficiency of DiD in the systems was determined upon separation of the NE or NCs from the free components in the aqueous medium. The analysis was done directly. Briefly, 1 mL of the non-isolated formulations was ultracentrifuged (Beckman Coulter, Optima L−90K, Brea, USA) at 112,202.7 g for 1 h at 15 °C. After the isolation the cream fractions were collected and resuspended with ultrapure water up to their initial volume. Then, the encapsulated DiD was extracted from the isolated systems by the following procedure: *i)* 100 µL of the isolated system was vortexed with 100 µL of acetonitrile for 1 min; *ii)* 100 µL of Triton™ X−100 were incorporated to the previous mixture and vortexed for 1 min; *iii)* Finally, samples were diluted with extra-acetonitrile, and the fluorescence emitted by the broken isolated nanosystems was analyzed using an EnVision Multilabel plate reader 2104−0010A (λ_{ex} = 644 nm, λ_{em} = 665 nm) in order to determine the amount of DiD associated to them. In addition, 1 mL of non-isolated systems were degraded following the same procedure and the total DiD concentration was determined in the same way as control. The encapsulation efficiency of DiD in the systems was expressed as percentage, and calculated dividing the amount of DiD determined in the isolated nanosystems by the total amount of DiD incorporated to them initially. The analysis was done in triplicate.

2.4. Colloidal stability in simulated intestinal fluid (SIF)

In order to evaluate the colloidal stability, size and changes in the ζ−potential were determined using a Malvern Zeta-sizer device (NanoZS, ZEN 3600, Malvern Instruments, Worcestershire, UK). In short, 30 µL of the systems were incubated with 970 µL of the corresponding medium under horizontal shaking at 37 °C, and for the size evaluation,

samples were analyzed at 0, 0.5, 1, 2, and 4 hours. Colloidal stability was studied in plain (without enzymes) and in normal SIF (USP XXIX). The SIF (1 % w/v pancreatin) medium was centrifuged 5 minutes at 5000 g at 5 °C using a Universal 32 R, Hettich Zentrifugen (Hettich Instruments) in order to eliminate the pancreatin aggregates, prior to the incubation of the nanocarriers. In addition, to check the changes in the surface charge of the systems, the same procedure was done and the ζ–potential determined after 1 hour of incubation.

2.5. Lipolysis assay

The potential effect of the nanosystems surface on their chemical degradation by the intestinal enzymes was evaluated using an acid-base titration. The lipases present in the medium degrade the triglycerides of the oily core and generate two fatty acids and one monoglyceride. The release of these fatty acids causes a decrease in the pH of the medium. Therefore, the titration of these fatty acids with NaOH will allow the quantification of the amount of triglycerides degraded by the enzymes after the incubation of the nanosystems with 1 % pancreatin SIF. The degradation of the NE without surfactants after 5 hours of incubation in SIF was set as 100 % degradation. For this study, a titrator TitroLine® alpha Plus (Scott Instruments, Germany) was used to evaluate the release of fatty acids using NaOH 0.01 N.

To perform the titration, on the one hand, 1 mL of formulation was mixed with 4 mL of SIF and its pH was adjusted to 6.8 with NaOH 0.01 N; on the other hand, a solution of 2 % (w/v) pancreatin in SIF was prepared under magnetic stirring and then centrifuged 5 minutes at 5000 g at 5 °C using a Universal 32 R, Hettich Zentrifugen (Hettich Instruments, Germany). After the centrifugation, the pH of 5 mL of undernatant was adjusted to 6.8 with NaOH 0.01 N. Then, these 5 mL were mixed with the 5 mL containing the system previously mixed with SIF, to a final pancreatin concentration of 1 %. The titration was done at 37 °C under continuous magnetic stirring.

2.6. Mucoadhesion studies

2.6.1. Dynamic light scattering

This method, based on a modification of a previously described technique [45], was designed as a fast bench screening assay to study the affinity of the systems for mucin, which is the main component of the mucus [27]. The study involved the analysis of the nanosystems size (expressed as the aggregation ratio $Size_{MUCIN}/Size_{SIF}$) and ζ–potential upon exposure to non-supplemented SIF diluted in water (1/25) containing increasing concentrations of mucin (1×10^{-4} to 1×10^{-1} % (w/v)). For this study, a Malvern Zeta-sizer device (NanoZS, ZEN 3600, Malvern Instruments, Worcestershire, UK) was used. The mucin threshold used was selected according to inherent limitations of the DLS. While

concentrations ≤ 1 x 10^{-1} had similar physicochemical properties as dispersion medium, higher mucin concentrations led to viscosity and turbidity issues that did not allow the direct comparison between both media (data not shown).

2.6.2. Fluorescence microscopy

This method, a modification of the method already published by Tachaprutinun et al. [46], allows the evaluation of the nanosystems interaction with a mucin film, as a complementary assay to determine the mucoadhesion of the prototypes as a function of their shell composition. This technique is based on the determination of the fluorescent-labeled nanosystems retention after their incubation with a mucin layer. Briefly, two series of glass bottom dishes were pretreated either with poly-D−lysine (to promote the adsorption of the mucin to the glass dish) or with a 25 mg/mL solution of PF127 (as negative control). Then 200 µL of a 5 % (w/v) mucin solution in diluted plain SIF (1/25) was added. After 8 hours of incubation, the excess of mucin or PF127 was removed by washing the glass bottom 5 times with ultrapure water, and letting it dry. Through this procedure, a superficial layer of mucin, bounded by electrostatic interactions to the poly-D−lysine, was created. Then, 200 µL of the different isolated DiD-loaded nanosystems were incubated onto the glass bottom during 2 hours. Finally, the non-muco-interactive nanosystem was eliminated by washing the glass bottom 3 times with ultrapure water. Photos of the glass dishes were taken with a 20X objective and the fluorescence intensity was determined (λ_{ex} ≈ 644 nm, λ_{em} ≈ 665 nm) using a microscope Leica AF6000 (Leica Microsystems, Germany). Given the well-known mucoadhesive properties of CS [38,47–49] we used, as a positive reference (100% mucoadhesion), the fluorescence emitted by the CS NCs without surfactants.

2.7. Mucodiffusion studies

2.7.1. Particle Tracking Analysis using porcine mucus

As model of the human intestinal mucosa, we used fresh porcine intestinal mucus obtained from the local slaughterhouse. NEs and NCs were fluorescently labeled by incorporating the lipophilic tracer DiD to the oil core during the formulation process. Briefly, 5 µL of nanosystem previously diluted in PBS 2 mM were mixed with 100 µL of mucus. Volumes of 10 µL of each sample were placed between a microscope slide and a cover glass in a chamber created by the placement of a 120 µm thick, double-sided adhesive sticker between slide and cover (Sigma). The Nikon microscope (Izasa Scientific, Spain) equipped with an Andor Zyla 4.2 camera and a PLAN APO 100X 1.4 oil-immersion objective was always focused at 12−16 µm above the cover glass. For each sample, more than 20 movies of 800 frames were recorded at a frame rate of 100 fps, obtaining more

than 100 trajectories per movie. The diffusion coefficient of each nanosystem was obtained off-line from the fitting of the mean square displacement ⟨MSD⟩ as a function of the time according to the following equation: $\langle MSD \rangle = 4D_e\tau^{\alpha}$ (*Eq. 1*), where D_e is the effective diffusion coefficient, α the anomalous exponent that gives information about the nature of the diffusion mode of the nanosystem in mucus and τ, the time scale, which is the time over which nanosystems are allow to move before calculating their displacement trajectories. The time scale was fixed at 1 second for these experiments (100 frames/s) [50–52].

The same procedure was performed using an aqueous solution of DiD at the sample concentration, and the results were analyzed to ensure that the signal observed did not originated from the released DiD.

2.7.2. Capillary in porcine mucus

To learn about the mucodiffusion of the systems from a macroscopic point of view, we adapted a capillary technique described elsewhere [53,54]. Briefly, borosilicate capillaries were filled at one end with intestinal porcine mucus obtained from the local slaughterhouse while the DiD-labeled formulations were slowly injected at the opposite end. Once the formulation came in contact with the porcine mucus, the diffusion of the nanosystems was studied using a fluorescence microscope Leica AF6000 (Leica Microsystems, Germany) by measuring at $\lambda_{ex} \approx 644$ nm and $\lambda_{em} \approx 665$ nm. The capillaries were maintained in a vertical position during the measurement.

By fitting of the fluorescence decay versus the distance, it was possible to calculate the mean penetration capacity of the systems through porcine mucus ($X_{1/2}$) using the following equation: $I_F = A + I_0 e^{-x/k}$ (*Eq. 2*), where I_F is the normalized fluorescence, *A* is the basal normalized fluorescence, I_0 the fluorescence at $X = 0$ (mucus/nanosystems interface), *X* is the distance from the mucus/nanosystems interface towards the mucus, and *k* is a decay constant that obeys: $k = \frac{X_{1/2}}{\ln 2}$ (*Eq. 3*), being $X_{1/2}$ the penetration capacity, which means the thickness (μm) of intestinal porcine mucus that allows the transport of 50 % of the nanosystems.

2.7. Statistical analysis

GraphPad Prism 7 program (California, USA) was used to perform the statistical analysis. Where applicable, and after confirmation of the normal distribution of data using the Shapiro-Wilk normality test, they were compared using the two-way ANOVA followed by a Fisher's LSD test, considering p-values lower than 0.05 as statistically significant.

3. Results and discussion

In this study, we analyzed nine different nanosystems in the form of nanoemulsions or nanocapsules, all of them having the same oily core but different shell composition. The shell was made of polymers (CS and PARG), surfactants (PF68 and PF127) and a combination of them. Specifically, we studied the effect of each specific combination on the colloidal stability, enzymatic degradation and mucoadhesion/mucodiffusion of these colloidal systems.

3.1. Physicochemical characterization of nanoemulsions and nanocapsules

The versatility of the core-shell polymeric NCs relies on the possibility to adapt the composition of the oily core to the nature of the cargo, and that of the polymeric shell to the administration route or target tissue [35,43,55–57]. Bearing this in mind, the first studies focused on the analysis of the effect of the polymer and the surfactant coating on the physicochemical properties of the systems. As shown in *Table 2*, the incorporation of either CS or PARG led to the charge inversion of the nanostructures, while their hydrodynamic mean sizes remained in the nanometric range with a low polydispersity index. These results indicated the efficient formation of a polymeric shell after the incubation of the NE with either polymer, most probably due to the attractive electrostatic interaction between the cationic polymer (either CS or PARG) and the negatively charged NE [35,39,55].

Regarding the influence of the non-ionic surfactant on the physicochemical properties of the three different nanosystems, the results in *Table 2* indicate that the addition of PF68 did not lead to a significant modification of their initial size and ζ−potential values. However, the incorporation of PF127 to the nanosystems led to different behaviors depending on their composition. An important decrease on the ζ−potential magnitude was observed in plain NE and PARG NCs when PF127 was incorporated, however, this reduction less marked in the case of CS NCs (*Table 2*). The different behaviour observed for both surfactants can be attributed to their different molecular structures (see *Table 1*). Although both Pluronics® share the same PEO_n−PPO_m−PEO_n architecture, PF68 presents two hydrophilic side arms with 75 × PEO monomers and a central hydrophobic block formed by 29 × PPO monomers (HLB ≈ 29), while PF127 has 100 × PEO units in its hydrophilic side arms and 65 × PPO units in the central hydrophobic block (HLB ≈ 22). The number of monomers in the hydrophilic side arms may influence the protective steric layer of the nanostructures [55,58], whereas the central hydrophobic block is expected to determine the interfacial adsorption of the surfactant as well as its ability to compete with

other components present at the oil/water interface [44,59,60]. In theory, the presence of non-ionic surfactants on the nanosystems surface should lead to a displacement of the shear plane (where the ζ−potential is defined) towards the aqueous phase, and, hence, to a reduction on the ζ−potential magnitude [58]. Bearing this in mind, our results would indicate a low incorporation of PF68 to the nanostructure irrespective of the shell composition, since its incorporation did not produce any significant change in the ζ−potential [32,55,61]. In contrast, the significant ζ−potential reduction in magnitude for both, NE and PARG NCs, when PF127 was used instead of PF68, could be an indication of its greater incorporation onto the oily core due to its higher lipophilicity. In the case of CS NCs, the lower but still significant reduction on the ζ−potential suggests a low incorporation of PF127.

Table 2. Physicochemical properties of nanoemulsions (NEs), chitosan (CS) and polyarginine (PARG) nanocapsules (NCs)*. All systems share the same Miglyol®812N/lecithin core (n ≥ 3).*
[Table 2]

3.2. Stability of nanoemulsions and nanocapsules in simulated intestinal fluid

We evaluated the role of the nanosystem surface composition on both, colloidal stability and resistance to the enzymatic degradation upon incubation in simulated intestinal fluid (SIF) USP XXIX. Given the complex composition of the intestinal medium, and in order to achieve a better understanding of the effect of each nanosystem surface component on the colloidal behaviour of the formulations, we first studied the size evolution of the systems in SIF supplemented or not with 1 % pancreatin.

As depicted in *Figure 2 (upper panel)*, both, surfactant-free and PF68-containing CS and PARG NCs, showed an immediate aggregation (CS NCs ≥ 1 µm and PARG NCs ≈ 750 nm) upon incubation in SIF without enzymes. These results correlate with the similar physicochemical properties of these nanosystems (no significant differences, *Table 2*), and agree with our hypothesis of a low incorporation of PF68 to the oil/water interface. On the contrary, the NCs formulated with PF127 were more stable. As expected, this effect was more noticeable in the case of PARG NCs than in the case of CS NCs, probably due to the lower incorporation of the surfactant onto the CS NCs.

Once the effect of the electrolytes present in the intestinal fluids has been established, we found important to understand the role of the intestinal enzymes in the colloidal stability of the systems. For this purpose, the previous stability assay was performed on normal SIF (supplemented with 1 % of pancreatin). As shown in *Figure 2 (lower panel)*, all systems presented a certain modification in size, which could be attributed to the enzymes adsorption [33,62,63]. The absence of a massive aggregation observed in this case might

be a consequence of the formation of an stabilizing coating of the particles/oily droplets by the enzymes present in the medium [64].

[Figure 2]

Figure 2. Colloidal stability in simulated intestinal fluid. *Hydrodynamic mean size of the NEs (black), CS NCs (red) and PARG NCs (blue) incubated either in SIF without enzymes (top) or in 1 % pancreatin supplemented SIF (bottom) (Error bars mean standard deviation; n ≥ 3).*

The DLVO theory states that the total potential of interaction (V_T) between two approaching particles can be expressed as $V_T = V_A + V_R$, where V_A is the attractive potential of interaction due to the Van der Waals forces and V_R is the repulsive electrostatic potential that depends on the ζ−potential magnitude [65]. Bearing this in mind, the evolution of the ζ−potential values upon incubation of the nanosystems in SIF with and without pancreatin was monitored (*Figure 3*) in order to elucidate if the stability profile of the nanosystems was driven by either electrostatic interactions or steric hindrances. In the absence of enzymes, it was found that NEs incubated in SIF suffered a minor reduction of their ζ−potential. Therefore, while the high negative ζ−potential observed in the case of non-coated and FP68-coated NEs (≈ −60 mV) could be responsible for their stability in plain SIF, in the case of the PF127-coated NE, whose ζ−potential was much lower in magnitude (≈ −23 mV), its stability would be mainly attributable to a steric stabilization provided by the PF127-coating, as previously reported [21,66,67]. In contrast, both types of NCs experienced a significant decrease in their ζ−potential in plain SIF, which was attributed to the reduced ionization of the–NH_3^+ groups ($pK_a \approx 8$) in this medium (pH 6.8), as compared to the one in the original pH of these formulations (≈ 4.5, *Table 2*) [55]. The ζ−potential decrease observed in the case of the NCs (≤ +15 mV, $p \leq 0.0001$) may result in a reduction of V_R (repulsive electrostatic potential) and, hence, in the instability in plain SIF of the non-sterically stabilized particles (*Figure 2*) [55,60,66]. Also, it could be assumed that the incorporation of PF127 to PARG NCs was high enough to lead to the steric stabilization of the nanosystem [33,62,63]. Finally, a generic observation is that upon incubation in SIF with pancreatin the surface charge of all systems becomes similar (≈ −15 ± 5 mV), a fact that could be due to their interaction with enzymes present in the medium and the formation of a stabilizing enzyme coating.

[Figure 3]

Figure 3. Surface charge of the nanosystem in different media. *ζ−potential (mV) of the NEs (black), CS NCs (red) and PARG NCs (blue) measured either in KCl 1 mM (closed bars), SIF without enzymes (sparse dashed bars) or 1 % pancreatin supplemented SIF (dashed bars) (Error bars mean standard deviation; n ≥ 3).*

3.3. Lipolysis of the oily core of nanoemulsions and nanocapsules

Another important aspect to consider is the potential protection that the different polymer/surfactant coatings confer to the nanosystems against enzimatic degradation.

Figure 4 shows the percentage of oily core degradation of the different systems when incubated in normal SIF in the presence of pancreatic lipase [19]. The degradation kinetics was qualitatively similar for the 9 tested systems showing an initial fast degradation (during the first 20 minutes), followed by a plateau for the rest of the experiment.

As expected, due to the important exposure to the enzymes of the oily core of the NE prepared without non-ionic surfactants, this was the formulation that presented the highest degradation by pancreatic enzymes (70 % in 20 minutes), being its area under the curve significantly higher than those corresponding to CS NCs ($p \leq 0.0001$) and PARG NCs ($p \leq 0.001$). This was mainly attributed to the interaction of the pancreatic lipase with the oily droplets [19,60,68], being this degradation slightly reduced by the CS and PARG coatings. We have speculated that this limited protective effect of the polymeric shell could be attributed to the presence of amylases, enzymes with the capacity of degrading CS through the α(1,4) glycosidic bond cleavage [69–71], and peptidases, enzymes capable of degrading PARG backbone through the peptide bond [68,72].

Our group has previously shown that PF68 can efficiently protect nanoparticles made of polylactic-co-glycolic acid (PLGA) from enzymatic degradation in SIF [58,72]. As depicted in *Figure 4*, the incorporation of PF68 did significantly slow down the degradation of the NE (70 % of degradation in 40 minutes) ($p \leq 0.0001$) and of the NCs (70 % of degradation in 60 minutes) ($p \leq 0.01$ for CS NCs and $p \leq 0.001$ for PARG NCs), although it did not prevent totally the action of the pancreatic lipase

The most resistant systems against enzymatic degradation were those formulated with PF127. While both, NE and PARG NCs, presented a maximum degradation of about 20 % after 2 hours of incubation in SIF; the percentage of degradation of CS NCs was close to 60 %. As discussed above, the surfactant protection effect depends on its capacity to be efficiently adsorbed and retained onto the nanosystems upon their incubation with enzymes. Considering the ζ−potential values from *Table 2* and the low degradation observed for NE and PARG NCs, it seems that PF127 was efficiently incorporated to the oil/water interface of both formulations. In addition, the low degradation observed in this case suggests that the surfactant was not displaced from the oil/water interface by the macromolecules present in SIF [21,59,67,73]. Accordingly, the significantly higher degradation observed for CS NCs ($p \leq 0.0001$ compared to both NE and PARG NCs) could be mainly attributed to a lower incorporation of PF127, but not to a displacement of the surfactant from the oil/water interface after incubation in SIF [21,73].

[Figure 4]

Figure 4. Lipolysis in simulated intestinal fluid. *Percentage of lipolysis of the NEs (black), CS NCs (red) and PARG NCs (blue) incubated in SIF. Degradation of the non-coated NE after 5 hours of incubation in SIF was set as 100 % of degradation (Error bars mean standard deviation; n ≥ 3).*

3.4. Mucoadhesion of nanoemulsions and nanocapsules

3.4.1. Dynamic light scattering

To be successful, in addition to overcoming the harsh intestinal environment, nanomedicines should diffuse across the intestinal mucosa and reach the intestinal epithelium [27,31]. Bearing this in mind, the role of the surface properties of our prototypes on their interaction with mucin was first analyzed according to a simple DLS-based procedure [27]. The analysis of the $Size_{MUCIN}/Size_{SIF}$ and the ζ−potential of the different systems in the presence of increasing amounts of mucin in SIF allowed us to classify the nanosystem-mucin interaction as follows: *i)* Strong interactions with mucin fibres may lead to the entrapment of the nanosystems within mucin meshes and, thus, to a subsequent increment in the size of nanosystems (aggregation) and their ζ−potential values are similar to the mucin charge; *ii)* The formation of a mucin coating around the nanosystems may be justified by the fact that their size remains invariable while their ζ−potential values are similar to the mucin charge ; *iii)* Muco-inert nanosystems will not experience variations in either size or ζ−potential when incubating with mucin fibres.

As shown in *Figure 5*, NE formulated without poloxamer presented a constant size for all mucin concentrations while the corresponding NCs suffered a mucin concentration-dependent aggregation induced by the interaction with mucin [64]. Parallel analysis of ζ−potential as function of the mucin concentration complemented the information obtained by size analysis. These results revealed that, despite the constant size displayed by the NE, the decrease in its ζ−potential magnitude with the mucin concentration towards those values observed for the pure mucin solution is a clear indicative of the interaction of the system with the mucin fibers.

In agreement with the results described above, formulations containing PF68 behaved like the formulations without surfactant. This is consistent with our hypothesis that the incorporation of this surfactant onto the oil/water interface is low, and it has a tendency to be displaced by other macromolecules with more affinity for this interface. Contrary to what was observed with PF68, PF127 formulations displayed a negligible size modification, but their ζ−potential was also dependent on the mucin concentration. These results indicate that PF127 cannot totally prevent the colloidal system from interacting with the mucin fibers. However, this interaction did not translate to an aggregation of the nanosystems.

[Figure 5]

Figure 5. Mucoadhesion assessed by the dynamic light scattering approach. *Hydrodynamic mean size increase, expressed as $Size_{Mucin}/Size_{SIF}$ ratio (top), and ζ−potential modification (bottom) of the NEs (black), CS*

NCs (red) and PARG NCs (blue) incubated in mucin solutions in diluted SIF (1/25) without enzymes with a concentration ranging from 1 x 10^{-4} to 1 x 10^{-1} % (w/v) (Error bars mean standard deviation; n ≥ 3).

3.4.2. Fluorescence microscopy

In order to understand better the effect that the shell composition of the systems has on their interaction with the intestinal mucosa, we studied the interaction of the nanosystems with a film of mucin immobilized on a glass bottom dish [46]. We incubated each system 2 hours with the mucin film and performed a semi-quantitative analysis of the retained nanosystems by fluorescent microscopy. For this purpose, the systems used in this assay were formulated with the fluorescent dye DiD in their oil core (all the systems presented an encapsulation efficiency ≥ 80 %; data not shown).

Based in the well-known mucoadhesive properties of CS [35,38,41,47–49,74], the fluorescence intensity measured for de CS NCs formulated without Pluronics® was set as 100 %. As shown in *Figure 6*, in the absence of poloxamer, the mucoadhesive behaviour was found to be clearly dependent on the polymeric shell. In the case of the NEs, a negligible amount of oily droplets were retained on the film mucin. This result suggest that despite the mucin-NE interaction observed by dynamic light scattering, this interaction is weak enough for the oily droplets to avoid being adsorbed to the mucin film. Both polymers, CS and PARG, substantially increase the mucoadhesion of the systems ($p \leq 0.0001$ compare to the NE). As expected, CS NCs, referred as 100 % mucoadhesion, showed the highest retention on the films, while PARG NCs had less affinity for the mucin (≈ 60 %; $p \leq 0.0005$ compared to CS NCs).

No significant effect was found on the mucoadhesive properties of the three nanosystems after the addition of PF68. This result agrees with the hypothetical low incorporation of this surfactant onto the oil/water interface. In contrast, the presence of PF127 significantly decreased these mucoadhesive properties for both NCs ($p \leq 0.05$), being the mucoadhesion displayed by the CS NCs significantly higher than that of PARG NCs ($p \leq 0.05$). This agrees with the more efficient incorporation of PF127 expected for the NE and the PARG NCs, than for the CS NCs. The effect of PF127 may be attributed to the more intense interaction of this Pluronic® with the oil droplets [44,60], which ended up in a more efficient coating against the interaction with the physiological macromolecules, such as mucin [44,60,61].

[Figure 6]

Figure 6. Mucoadhesion assessed by the fluorescence microscopy approach. *Adhesion percentage upon incubation with a mucin film of the NEs (black), CS NCs (red) and PARG NCs (blue) compared to the non-coated CS NCs (set as 100 %) (Error bars mean standard deviation; n ≥ 3).*

3.5. Mucodiffusion of nanoemulsions and nanocapsules

Once the nanosystems are captured by the intestinal mucus the next step is their diffusion across the mucus blanket that covers the intestinal epithelium. The nanosystems must be mucodiffusive enough to avoid being removed together with the loosely adherent mucus by the mucus clearance process and to reach and pass through the tightly bound mucus to finally be able to interact with the intestinal cells [26]. This diffusion was the focus of the last set of experiments, the analysis of the mucodiffusion capacity of the systems as a function of their specific surface composition. This analysis was performed from both microscopic and macroscopic points of view using intestinal porcine mucus as mucus model [75].

3.5.1. Particle Tracking Analysis using porcine mucus

Particle tracking was selected as the experimental technique used to evaluate the diffusion coefficient of the prototypes in intestinal mucus from a microscopic point of view. With this technique, the fitting of the mean square displacement of the particles ⟨MDS⟩ as a function of the time using the following equation: $\langle MSD \rangle = 4D_e\tau^{\alpha}$ (*Eq. 1*), allowed the calculation of the effective diffusion coefficient (D_e) of each individual particle, being α an indicative value about the nature of the diffusion mode of the nanoparticles in mucus and τ (time scale) the time over which particles were allowed to move before calculating their displacement trajectories (1 second, 100 frames/s) [50–52].

Figure 7 shows the distribution of the effective diffusion coefficient (D_e) of each individual particle/oily droplet of the nanosystems in both, intestinal porcine mucus and PBS calculated as a time scale of 1 second. Prototypes formulated without non-ionic surfactants displayed a clear reduction on their mobility once incubated in mucus. This is in line with our previous results that showed that all these systems displayed, to some extent, a clear interaction with mucin. Incorporation of PF68 to the prototypes did not have a clear effect on their diffusion capacity in mucus. Finally, the inclusion of PF127 was found to have a different effect depending on the prototype. While for CS and PARG NCs, this surfactant did not display a clear modification of their diffusion capacity, the NE showed a remarkable displacement of the oily droplets population towards higher diffusion values in mucus.

[Figure 7]

Figure 7. Mucodiffusion assessed by multiple particle tracking analysis. *Histogram of the effective diffusion coefficient (D_e) of the different nanosystems tested in intestinal porcine mucus (continuous line) and in PBS (dotted line) calculated at a time scale of 1 second. Non-coated (left), PF68-coated (middle) and PF127-coated (right) NEs (black), CS NCs (red) and PARG NCs (blue) (number of batches analyzed n = 3; n ≥ 1000 nanosystems).*

All these data were analyzed in depth by calculation of the mean effective diffusion coefficient (mean of the D_e of each individual nanosystem) of each prototype (*Figure 8*) [50,51]. No significant differences ($p \leq 0.05$) were found in the mean effective diffusion coefficient displayed by the non-coated formulations, resulting all of them (NE and NCs) highly retained in the mucus matrix. These results could be attributed to the hydrophobic character of the NE and the positive surface charge of CS and PARG. Both characteristics are expected to promote the interaction of the formulation with the mucin fibers present in the intestinal porcine mucus [34,35,38,41,44,60].

The incorporation of PF68 resulted in a similar behavior for the three nanosystems, with no significant differences being observed among them and with the non-coated formulations ($p \leq 0.05$). This could be attributed to the low association of this surfactant to the nanosystems, as highlighted before. In fact, the adsorption of PEG derivatives with a PEG−MW in the 5−10 kDa range, normally results in an enhancement of the mucodiffusion properties [51]. However, to achieve this goal, it is necessary to create a homogeneous and dense enough coating [44,76]. If the coating is not thick enough, it may lead to the entrapment of the nanostructure in the mucin mesh of the mucus [44,76].

The use of PF127 led to a remarkable improvement in the mucodiffusion capacity of the NE ($p \leq 0.0001$), with a mean diffusion coefficient of 1.9×10^{-2} μm^2/sec. These results are indicative of a better coating of the NE by this non-ionic surfactant [44,76]. However, this significant improvement was not observed in the case of the NCs, where it seems, that it was not possible to obtain a dense and homogeneous coating due to the presence of the CS or PARG polymers. As previously mentioned, the mucodiffusion capacity of the colloidal systems is strongly dependent on the coating density of the nanosystem, meaning that if the non-ionic surfactant coating is not perfectly homogeneous, it can result in a retention of the nanosystem in the mucus mesh [44,76].

[Figure 8]

Figure 8. Mucodiffusion assessed by multiple particle tracking analysis. *Mean effective diffusion coefficient of the non-coated, PF68-coated, and PF127-coated NEs (black), CS NCs (red) and PARG NCs (blue) calculated from their trajectories in porcine intestinal mucus at 37 °C at a time scale of 1 second (Error bars mean standard deviation; number of batches analyzed n = 3; n ≥ 1000 nanosystems).*

3.5.2. Capillary in porcine mucus

The previously discussed mucodiffusion microscopic assay was complemented by a macroscopic analysis, where the penetration profile of each nanosystem across a capillary filled with porcine intestinal mucus was also determined. The results in *Figure 9* show the mean penetration capacity ($X_{1/2}$), which means the thickness (μm) of intestinal porcine mucus that allows the transport of 50 % of the nanosystems. Overall, the results followed

the same trend found using particle tracking analysis (*Figure 8*), although some slight differences were observed. This distinct behavior could be attributable to the different concentration of nanosystem used in both procedures, being either not diluted for the capillary technique or 100-fold diluted for particle tracking analysis. These results showed that in the absence of poloxamer PARG NCs displayed the highest mucodiffusive properties ($p \leq 0.0001$), being the slighter cationic character of the PARG NCs ($p \leq 0.05$) probably the reason behind the lower retention of these NCs in the intestinal porcine mucus mesh ($p \leq 0.0001$) [26]. In agreement with the conclusions extracted from the nanoparticle tracking analysis, the low incorporation of PF68 in both NE and NCs did not result in an improved mucodiffusion of these nanosystems. In the same line, results showed the non-effective incorporation of PF127 in presence of CS and PARG and highlighted the important effect of PF127 on the mucodiffusion of the nanoemulsions [44,51,76].

[Figure 9]

Figure 9. Mucodiffusion assessed by the capillary approach. *Mean penetration capacity ($X_{1/2}$) of the non-coated, PF68-coated and PF127-coated NEs (black), CS NCs (red) and PARG NCs (blue) according to their penetration profile through a capillary filled with porcine mucus at 37 °C (Error bars mean standard deviation; n ≥ 3).*

Overall, these data suggest that the use of PF127 may be a strategy to improve the capacity of a nanosystem to overcome the multiple barriers associated to the oral modality of administration, i.e. colloidal stability, resistance against enzymatic degradation and intestinal mucus interaction/diffusion. However, when using this approach, one must take into account that the incorporation of this surfactant onto the surface of the nanosystem may interfere with other constituents present in the nanosystems shell.

4. Conclusions

Our results show that the interaction of nanosystems with biological barriers is dependent on their surface composition and that the contribution of each component can be affected by the presence of other components. Specifically, while the presence of PF127 alone contributes deeply to the stability of the formulation, and its capacity to diffuse across intestinal mucus, its use in the presence of CS or PARG had a limited effect on the formulation performance. In brief, these results highlight the need of a specifically engineered rational design of the nanocarriers in order for them to fulfill the adequate requirements for their performance as oral drug delivery vehicles. Ultimately, these data also emphasize the value of a proper characterization of the nanocarriers in line with their expected biological behavior.

Acknowledgements

The authors acknowledge financial support from the TRANS-INT European Consortium −FP7, under grant agreement No. 281035 and the Xunta de Galicia (Competitive Reference Groups -FEDER Funds; Ref 2014/043). Irene Santalices acknowledges a predoctoral grant from the FPU program (No. FPU13/02015) from the Ministry of Education, Culture and Sports, MECD, Spain. The authors acknowledge Servier for providing Servier Medical Art (http://smart.servier.com/), being the small intestine, intestinal villi and laboratory material and equipment (https://creativecommons.org/licenses/by/3.0/) modified from the original work and used for the creation of the *graphical abstract* and *Figure 1*.

Conflict of interest

The authors declare that there are no competing interests with the subject matter or materials discussed in the manuscript.

References

[1] M. Koziolek, M. Grimm, F. Schneider, P. Jedamzik, M. Sager, J.-P. Kühn, W. Siegmund, W. Weitschies, Navigating the human gastrointestinal tract for oral drug delivery: uncharted waters and new frontiers, Adv. Drug Deliv. Rev. 101 (2016) 75–88. doi:10.1016/j.addr.2016.03.009.

[2] A.L. Smart, S. Gaisford, A.W. Basit, Oral peptide and protein delivery: intestinal obstacles and commercial prospects, Expert Opin. Drug Deliv. 11 (2014) 1323–1335. doi:10.1517/17425247.2014.917077.

[3] M. Morishita, N.A. Peppas, Is the oral route possible for peptide and protein drug delivery?, Drug Discov. Today. 11 (2006) 905–910. doi:10.1016/j.drudis.2006.08.005.

[4] K. Park, I.C. Kwon, K. Park, Oral protein delivery: Current status and future prospect, React. Funct. Polym. 71 (2011) 280–287. doi:10.1016/j.reactfunctpolym.2010.10.002.

[5] E. Moroz, S. Matoori, J.-C. Leroux, Oral delivery of macromolecular drugs: where we are after almost 100 years of attempts, Adv. Drug Deliv. Rev. 101 (2016) 108–121. doi:10.1016/j.addr.2016.01.010.

[6] S.R. Hwang, Y. Byun, Advances in oral macromolecular drug delivery, Expert Opin. Drug Deliv. 11 (2014) 1955–1967. doi:10.1517/17425247.2014.945420.

[7] S. Maher, R.J. Mrsny, D.J. Brayden, Intestinal permeation enhancers for oral peptide delivery, Adv. Drug Deliv. Rev. 106 (2016) 277–319. doi:10.1016/j.addr.2016.06.005.

[8] B.F. Choonara, Y.E. Choonara, P. Kumar, D. Bijukumar, L.C. du Toit, V. Pillay, A review of advanced oral drug delivery technologies facilitating the protection and absorption of protein and peptide molecules, Biotechnol. Adv. 32 (2014) 1269–1282. doi:10.1016/j.biotechadv.2014.07.006.

[9] E.P. Herrero, M.J. Alonso, N. Csaba, Polymer-based oral peptide nanomedicines, Ther. Deliv. 3 (2012) 657–668. doi:10.4155/tde.12.40.

[10] K.B. Ryan, S. Maher, D.J. Brayden, C.M. O'Driscoll, Nanostructures overcoming the intestinal barrier: drug delivery strategies, in: M.J. Alonso, N. Csaba (Eds.), Nanostructured Biomater. Overcoming Biol. Barriers, Royal Society of Chemistry, 2012: pp. 63–91.

[11] I. Santalices, A. Gonella, D. Torres, M.J. Alonso, Advances on the formulation of proteins using

nanotechnologies, J. Drug Deliv. Sci. Technol. 42 (2017) 155–180. doi:10.1016/j.jddst.2017.06.018.
[12] M.J. Alonso, Nanomedicines for overcoming biological barriers, Biomed. Pharmacother. 58 (2004) 168–172. doi:10.1016/j.biopha.2004.01.007.
[13] Z. Niu, I. Conejos-Sánchez, B.T. Griffin, C.M. O'Driscoll, M.J. Alonso, Lipid-based nanocarriers for oral peptide delivery, Adv. Drug Deliv. Rev. 106 (2016) 337–354. doi:10.1016/j.addr.2016.04.001.
[14] W. Suchaoin, A. Bernkop-Schnürch, Nanocarriers protecting toward an intestinal pre-uptake metabolism, Nanomedicine. 12 (2017) 255–269. doi:10.2217/nnm-2016-0331.
[15] T.A.S. Aguirre, D. Teijeiro-Osorio, M. Rosa, I.S. Coulter, M.J. Alonso, D.J. Brayden, Current status of selected oral peptide technologies in advanced preclinical development and in clinical trials, Adv. Drug Deliv. Rev. 106 (2016) 223–241. doi:10.1016/j.addr.2016.02.004.
[16] C. Liu, Y. Kou, X. Zhang, H. Cheng, X. Chen, S. Mao, Strategies and industrial perspectives to improve oral absorption of biological macromolecules, Expert Opin. Drug Deliv. 15 (2018) 223–233. doi:10.1080/17425247.2017.1395853.
[17] H.R. Lakkireddy, M. Urmann, M. Besenius, U. Werner, T. Haack, P. Brun, J. Alié, B. Illel, L. Hortala, R. Vogel, D. Bazile, Oral delivery of diabetes peptides — Comparing standard formulations incorporating functional excipients and nanotechnologies in the translational context, Adv. Drug Deliv. Rev. 106 (2016) 196–222. doi:10.1016/j.addr.2016.02.011.
[18] L. Rosenmayr-Templeton, The oral delivery of peptides and proteins: established versus recently patented approaches, Pharm. Pat. Anal. 2 (2013) 125–145. doi:10.4155/ppa.12.75.
[19] R. Devraj, H.D. Williams, D.B. Warren, A. Mullertz, C.J.H. Porter, C.W. Pouton, In vitro digestion testing of lipid-based delivery systems: calcium ions combine with fatty acids liberated from triglyceride rich lipid solutions to form soaps and reduce the solubilization capacity of colloidal digestion products, Int. J. Pharm. 441 (2013) 323–333. doi:10.1016/j.ijpharm.2012.11.024.
[20] M. Wulff-Pérez, M.J. Gálvez-Ruíz, J. de Vicente, A. Martín-Rodríguez, Delaying lipid digestion through steric surfactant Pluronic F68: a novel in vitro approach, Food Res. Int. 43 (2010) 1629–1633. doi:10.1016/j.foodres.2010.05.006.
[21] M. Wulff-Pérez, J. de Vicente, A. Martín-Rodríguez, M.J. Gálvez-Ruiz, Controlling lipolysis through steric surfactants: new insights on the controlled degradation of submicron emulsions after oral and intravenous administration, Int. J. Pharm. 423 (2012) 161–166. doi:10.1016/j.ijpharm.2011.12.025.
[22] L. Serra, J. Doménech, N.A. Peppas, Engineering design and molecular dynamics of mucoadhesive drug delivery systems as targeting agents, Eur. J. Pharm. Biopharm. 71 (2009) 519–528. doi:10.1016/j.ejpb.2008.09.022.
[23] F.J.O. Varum, F. Veiga, J.S. Sousa, A.W. Basit, An investigation into the role of mucus thickness on mucoadhesion in the gastrointestinal tract of pig, Eur. J. Pharm. Sci. 40 (2010) 335–341. doi:10.1016/j.ejps.2010.04.007.
[24] Y.-Y. Wang, S.K. Lai, C. So, C. Schneider, R. Cone, J. Hanes, Mucoadhesive nanoparticles may disrupt the protective human mucus barrier by altering its microstructure, PLoS One. 6 (2011) e21547. doi:10.1371/journal.pone.0021547.
[25] C. Atuma, V. Strugala, A. Allen, L. Holm, The adherent gastrointestinal mucus gel layer: thickness and physical state in vivo, Am. J. Physiol. Gastrointest. Liver Physiol. 280 (2001) G922–G929. http://www.ncbi.nlm.nih.gov/pubmed/11292601.
[26] L.M. Ensign, R. Cone, J. Hanes, Oral drug delivery with polymeric nanoparticles: the gastrointestinal mucus barriers, Adv. Drug Deliv. Rev. 64 (2012) 557–570. doi:10.1016/j.addr.2011.12.009.
[27] S.K. Lai, Y.-Y. Wang, D. Wirtz, J. Hanes, Micro- and macrorheology of mucus, Adv. Drug Deliv. Rev. 61 (2009) 86–100. doi:10.1016/j.addr.2008.09.012.
[28] H. Takeuchi, Y. Matsui, H. Yamamoto, Y. Kawashima, Mucoadhesive properties of carbopol or

chitosan-coated liposomes and their effectiveness in the oral administration of calcitonin to rats, J. Control. Release. 86 (2003) 235–242. doi:10.1016/S0168-3659(02)00411-X.

[29] J.D. Smart, The basics and underlying mechanisms of mucoadhesion, Adv. Drug Deliv. Rev. 57 (2005) 1556–1568. doi:10.1016/j.addr.2005.07.001.

[30] S.E. Harding, Trends in muco-adhesive analysis, Trends Food Sci. Technol. 17 (2006) 255–262. doi:10.1016/j.tifs.2005.12.007.

[31] S.K. Lai, Y.-Y. Wang, J. Hanes, Mucus-penetrating nanoparticles for drug and gene delivery to mucosal tissues, Adv. Drug Deliv. Rev. 61 (2009) 158–171. doi:10.1016/j.addr.2008.11.002.

[32] M. Yang, S.K. Lai, Y.-Y. Wang, W. Zhong, C. Happe, M. Zhang, J. Fu, J. Hanes, Biodegradable nanoparticles composed entirely of safe materials that rapidly penetrate human mucus, Angew. Chemie - Int. Ed. 50 (2011) 2597–2600. doi:10.1002/anie.201006849.

[33] C. Prego, D. Torres, E. Fernandez-Megia, R. Novoa-Carballal, E. Quiñoá, M.J. Alonso, Chitosan-PEG nanocapsules as new carriers for oral peptide delivery: effect of chitosan pegylation degree, J. Control. Release. 111 (2006) 299–308. doi:10.1016/j.jconrel.2005.12.015.

[34] C. Prego, D. Torres, M.J. Alonso, Chitosan nanocapsules as carriers for oral peptide delivery: effect of chitosan molecular weight and type of salt on the in vitro behaviour and in vivo effectiveness, J. Nanosci. Nanotechnol. 6 (2006) 2921–2928. doi:10.1166/jnn.2006.429.

[35] C. Prego, M. Fabre, D. Torres, M.J. Alonso, Efficacy and mechanism of action of chitosan nanocapsules for oral peptide delivery, Pharm. Res. 23 (2006) 549–556. doi:10.1007/s11095-006-9570-8.

[36] Z. Niu, E. Tedesco, F. Benetti, A. Mabondzo, I.M. Montagner, I. Marigo, D. Gonzalez-Touceda, S. Tovar, C. Diéguez, M.J. Santander-Ortega, M.J. Alonso, Rational design of polyarginine nanocapsules intended to help peptides overcoming intestinal barriers, J. Control. Release. 263 (2016) 4–17. doi:10.1016/j.jconrel.2017.02.024.

[37] P. Calvo, C. Remuñán-López, J.L. Vila-Jato, M.J. Alonso, Development of positively charged colloidal drug carriers: chitosan-coated polyester nanocapsules and submicron-emulsions, Colloid Polym. Sci. 275 (1997) 46–53. doi:10.1007/s003960050050.

[38] C. Prego, D. Torres, M.J. Alonso, The potential of chitosan for the oral administration of peptides, Expert Opin. Drug Deliv. 2 (2005) 843–854. doi:10.1517/17425247.2.5.843.

[39] M. V. Lozano, G. Lollo, M. Alonso-Nocelo, J. Brea, A. Vidal, D. Torres, M.J. Alonso, Polyarginine nanocapsules: a new platform for intracellular drug delivery, J. Nanoparticle Res. 15 (2013) 15:1515. doi:10.1007/s11051-013-1515-7.

[40] J. das Neves, M.F. Bahia, M.M. Amiji, B. Sarmento, Mucoadhesive nanomedicines: characterization and modulation of mucoadhesion at the nanoscale, Expert Opin. Drug Deliv. 8 (2011) 1085–1104. doi:10.1517/17425247.2011.586334.

[41] C. Prego, M. García, D. Torres, M.J. Alonso, Transmucosal macromolecular drug delivery, J. Control. Release. 101 (2005) 151–162. doi:10.1016/j.jconrel.2004.07.030.

[42] P. Hervella, G. Lollo, F. Oyarzñun-Ampuero, G. Rivera, D. Torres, M.J. Alonso, Nanocapsules as carriers for the transport and targeted delivery of bioactive molecules, Pan Stanford Publishing Pte. Ltd., 2011. doi:10.1201/b11035-4.

[43] F.M. Goycoolea, A. Valle-Gallego, R. Stefani, B. Menchicchi, L. David, C. Rochas, M.J. Santander-Ortega, M.J. Alonso, Chitosan-based nanocapsules: physical characterization, stability in biological media and capsaicin encapsulation, Colloid Polym. Sci. 290 (2012) 1423–1434. doi:10.1007/s00396-012-2669-z.

[44] M.J. Santander-Ortega, M. Plaza-Oliver, V. Rodríguez-Robledo, L. Castro-Vázquez, N. Villaseca-González, J. González-Fuentes, E.L. Cano, P. Marcos, M. V. Lozano, M.M. Arroyo-Jiménez, PEGylated

nanoemulsions for oral delivery: role of the inner core on the final fate of the formulation, Langmuir. 33 (2017) 4269–4279. doi:10.1021/acs.langmuir.7b00351.

[45] W. Sajomsang, P. Gonil, U.R. Ruktanonchai, N. Pimpha, I. Sramala, O. Nuchuchua, S. Saesoo, S. Chaleawlert-umpon, S. Puttipipatkhachorn, Self-aggregates formation and mucoadhesive property of water-soluble β-cyclodextrin grafted with chitosan, Int. J. Biol. Macromol. 48 (2011) 589–595. doi:10.1016/j.ijbiomac.2011.01.028.

[46] A. Tachaprutinun, P. Pan-In, S. Wanichwecharungruang, Mucosa-plate for direct evaluation of mucoadhesion of drug carriers, Int. J. Pharm. 441 (2013) 801–808. doi:10.1016/j.ijpharm.2012.12.028.

[47] V. V. Khutoryanskiy, Advances in mucoadhesion and mucoadhesive polymers, Macromol. Biosci. 11 (2011) 748–764. doi:10.1002/mabi.201000388.

[48] M. Garcia-Fuentes, M.J. Alonso, Chitosan-based drug nanocarriers: where do we stand?, J. Control. Release. 161 (2012) 496–504. doi:10.1016/j.jconrel.2012.03.017.

[49] S. Roy, K. Pal, A. Anis, K. Pramanik, B. Prabhakar, Polymers in mucoadhesive drug-delivery systems: a brief note, Des. Monomers Polym. 12 (2009) 483–495. doi:10.1163/138577209X12478283327236.

[50] E. Zagato, K. Forier, T. Martens, K. Neyts, J. Demeester, S. De Smedt, K. Remaut, K. Braeckmans, Single-particle tracking for studying nanomaterial dynamics: applications and fundamentals in drug delivery, Nanomedicine. 9 (2014) 913–927. doi:10.2217/nnm.14.43.

[51] B.S. Schuster, L.M. Ensign, D.B. Allan, J.S. Suk, J. Hanes, Particle tracking in drug and gene delivery research: state-of-the-art applications and methods, Adv. Drug Deliv. Rev. 91 (2015) 70–91. doi:10.1016/j.addr.2015.03.017.

[52] J. Suh, M. Dawson, J. Hanes, Real-time multiple-particle tracking: Applications to drug and gene delivery, Adv. Drug Deliv. Rev. 57 (2005) 63–78. doi:10.1016/j.addr.2004.06.001.

[53] J. Kirch, A. Schneider, B. Abou, A. Hopf, U.F. Schaefer, M. Schneider, C. Schall, C. Wagner, C.-M. Lehr, Optical tweezers reveal relationship between microstructure and nanoparticle penetration of pulmonary mucus, Proc. Natl. Acad. Sci. 109 (2012) 18355–18360. doi:10.1073/pnas.1214066109.

[54] M. Kaipel, A. Wagner, E. Wassermann, K. Vorauer-Uhl, R. Kellner, H. Redl, H. Katinger, R. Ullrich, Increased biological half-life of aerosolized liposomal recombinant human Cu/Zn superoxide dismutase in pigs, J. Aerosol Med. Pulm. Drug Deliv. 21 (2008) 281–290. doi:10.1089/jamp.2007.0667.

[55] M.J. Santander-Ortega, M. V. Lozano-López, D. Bastos-González, J.M. Peula-García, J.L. Ortega-Vinuesa, Novel core-shell lipid-chitosan and lipid-poloxamer nanocapsules: Stability by hydration forces, Colloid Polym. Sci. 288 (2010) 159–172. doi:10.1007/s00396-009-2132-y.

[56] M.J. Santander-Ortega, J.M. Peula-García, F.M. Goycoolea, J.L. Ortega-Vinuesa, Chitosan nanocapsules: effect of chitosan molecular weight and acetylation degree on electrokinetic behaviour and colloidal stability, Colloids Surfaces B Biointerfaces. 82 (2011) 571–580. doi:10.1016/j.colsurfb.2010.10.019.

[57] D. Torrecilla, M. V. Lozano, E. Lallana, J.I. Neissa, R. Novoa-Carballal, A. Vidal, E. Fernandez-Megia, D. Torres, R. Riguera, M.J. Alonso, F. Dominguez, Anti-tumor efficacy of chitosan-g-poly(ethylene glycol) nanocapsules containing docetaxel: anti-TMEFF-2 functionalized nanocapsules vs. non-functionalized nanocapsules, Eur. J. Pharm. Biopharm. 83 (2013) 330–337. doi:10.1016/j.ejpb.2012.10.017.

[58] M.J. Santander-Ortega, A.B. Jódar-Reyes, N. Csaba, D. Bastos-González, J.L. Ortega-Vinuesa, Colloidal stability of Pluronic F68-coated PLGA nanoparticles: a variety of stabilisation mechanisms, J. Colloid Interface Sci. 302 (2006) 522–529. doi:10.1016/j.jcis.2006.07.031.

[59] A. Torcello-Gómez, J. Maldonado-Valderrama, J. de Vicente, M.A. Cabrerizo-Vílchez, M.J. Gálvez-

Ruiz, A. Martín-Rodríguez, Investigating the effect of surfactants on lipase interfacial behaviour in the presence of bile salts, Food Hydrocoll. 25 (2011) 809–816. doi:10.1016/j.foodhyd.2010.09.007.

[60] M. Plaza-Oliver, J. Fernández Sainz de Baranda, V. Rodríguez Robledo, L. Castro-Vázquez, J. Gonzalez-Fuentes, P. Marcos, M. V. Lozano, M.J. Santander-Ortega, M.M. Arroyo-Jimenez, Design of the interface of edible nanoemulsions to modulate the bioaccessibility of neuroprotective antioxidants, Int. J. Pharm. 490 (2015) 209–218. doi:10.1016/j.ijpharm.2015.05.031.

[61] Y.-Y. Wang, S.K. Lai, J.S. Suk, A. Pace, R. Cone, J. Hanes, Addressing the PEG mucoadhesivity paradox to engineer nanoparticles that "slip" through the human mucus barrier, Angew. Chemie - Int. Ed. 47 (2008) 9726–9729. doi:10.1002/anie.200803526.

[62] M. Tobío, A. Sánchez, A. Vila, I. Soriano, C. Evora, J.. J. Vila-Jato, M.. M. Alonso, The role of PEG on the stability in digestive fluids and in vivo fate of PEG-PLA nanoparticles following oral administration, Colloids Surfaces B Biointerfaces. 18 (2000) 315–323. doi:10.1016/S0927-7765(99)00157-5.

[63] M. García-Fuentes, D. Torres, M.J. Alonso, Design of lipid nanoparticles for the oral delivery of hydrophilic macromolecules, Colloids Surfaces B Biointerfaces. 27 (2002) 159–168. doi:10.1016/S0927-7765(02)00053-X.

[64] M. Tirado-Miranda, A. Schmitt, J. Callejas-Fernández, A. Fernández-Barbero, The aggregation behaviour of protein-coated particles: a light scattering study, Eur. Biophys. J. 32 (2003) 128–36. doi:10.1007/s00249-002-0275-6.

[65] J.A. Bernate, Vector chromatography of suspendedparticles in 1D-periodic systems, ProQuest LLC, 2012.

[66] M.J. Santander-Ortega, N. Csaba, M.J. Alonso, J.L. Ortega-Vinuesa, D. Bastos-González, Stability and physicochemical characteristics of PLGA, PLGA: poloxamer and PLGA: poloxamine blend nanoparticles: a comparative study, Colloids Surfaces A Physicochem. Eng. Asp. 296 (2007) 132–140. doi:10.1016/j.colsurfa.2006.09.036.

[67] C. Olbrich, R.H. Müller, Enzymatic degradation of SLN-effect of surfactant and surfactant mixtures, Int. J. Pharm. 180 (1999) 31–39. doi:10.1016/S0378-5173(98)00404-9.

[68] F.B. Landry, D. V. Bazile, G. Spenlehauer, M. Veillard, J. Kreuter, Degradation of poly (D,L-lactic acid) nanoparticles coated with albumin in model digestive fluids (USP XXII), Biomaterials. 17 (1996) 715–723. doi:10.1016/0142-9612(96)86742-1.

[69] O. Etienne, A. Schneider, C. Taddei, L. Richert, P. Schaaf, J.-C. Voegel, C. Egles, C. Picart, Degradability of polysaccharides multilayer films in the oral environment: an in vitro and in vivo study, Biomacromolecules. 6 (2005) 726–733. doi:10.1021/bm049425u.

[70] R.A.A. Muzzarelli, Human enzymatic activities related to the therapeutic administration of chitin derivatives, Cell. Mol. Life Sci. 53 (1997) 131–140. doi:10.1007/PL00000584.

[71] H. Zhang, Y. Du, X. Yu, M. Mitsutomi, S. Aiba, Preparation of chitooligosaccharides from chitosan by a complex enzyme, Carbohydr. Res. 320 (1999) 257–260. doi:10.1016/S0008-6215(99)00154-8.

[72] M.J. Santander-Ortega, D. Bastos-González, J.L. Ortega-Vinuesa, M.J. Alonso, Insulin-loaded PLGA nanoparticles for oral administration: an in vitro physico-chemical characterization, J. Biomed. Nanotechnol. 5 (2009) 45–53. doi:10.1166/jbn.2009.022.

[73] A. Torcello-Gómez, J. Maldonado-Valderrama, A.B. Jódar-Reyes, T.J. Foster, Interactions between Pluronics (F127 and F68) and bile salts (NaTDC) in the aqueous phase and the interface of oil-in-water emulsions, Langmuir. 29 (2013) 2520–2529. doi:10.1021/la3044335.

[74] C. Prego, D. Torres, M.J. Alonso, Chitosan nanocapsules: a new carrier for nasal peptide delivery, J. Drug Deliv. Sci. Technol. 16 (2006) 331–337. doi:10.1016/S1773-2247(06)50061-9.

[75] A.C. Groo, F. Lagarce, Mucus models to evaluate nanomedicines for diffusion, Drug Discov. Today. 19

(2014) 1097–1108. doi:10.1016/j.drudis.2014.01.011.

[76] Q. Xu, L.M. Ensign, N.J. Boylan, A. Schön, X. Gong, J.C. Yang, N.W. Lamb, S. Cai, T. Yu, E. Freire, J. Hanes, Impact of surface polyethylene glycol (PEG) density on biodegradable nanoparticle transport in mucus ex vivo and distribution in vivo, ACS Nano. 9 (2015) 9217–9227. doi:10.1021/acsnano.5b03876.

Table 1: Chemical structure and main characteristics of Pluronic®F68 and Pluronic®F127*. PEO: polyethylene oxide unit; PPO: propylene oxide unit. MW: molecular weight. HLB: hydrophilia-lipophilia balance.*

	$HO(CH_2CH_2O)_n(CHCH_2O)_m(CH_2CH_2O)_nH$ CH_3	
	Pluronic®F68	Pluronic®F127
n (PEO)	75	100
m (PPO)	30	65
MW (KDa)	8.4	12.6
HLB	29	22

Table 2. Physicochemical properties of nanoemulsions (NEs), chitosan (CS) and polyarginine (PARG) nanocapsules (NCs)*. All systems share the same Miglyol®812N/lecithin core (n ≥ 3).*

Polymeric Coating	Surfactant Coating	Final formulation pH	Size (nm)	PdI	ζ–Potential (mV)
-------- (NEs)	-----	5.3 ± 0.1	179 ± 15	0.1	−54 ± 1
	PF68	5.1 ± 0.1	172 ± 02	0.1	−54 ± 3
	PF127	5.2 ± 0.1	174 ± 04	0.1	−30 ± 3[a]
CS (NCs)	-----	4.8 ± 0.2	380 ± 19	0.3	+47 ± 3
	PF68	4.7 ± 0.1	383 ± 18	0.3	+49 ± 1
	PF127	4.8 ± 0.1	327 ± 12 [a]	0.3	+42 ± 2[b]
PARG (NCs)	-----	4.3 ± 0.1	188 ± 05	0.1	+43 ± 1
	PF68	4.3 ± 0.1	185 ± 03	0.1	+45 ± 1
	PF127	4.4 ± 0.1	183 ± 04	0.1	+27 ± 2[a]

Two-way ANOVA followed by a Fisher's LSD test were applied for the statistical analysis ($p < 0.05$). [a]Significantly different compared to both, the formulation without non-ionic surfactant and to the formulation with PF68 ($p \leq 0.0001$); [b]Significantly different compared to the formulation without non-ionic surfactant ($p \leq 0.01$) and to the formulation with PF68 ($p \leq 0.001$).

Graphical abstract

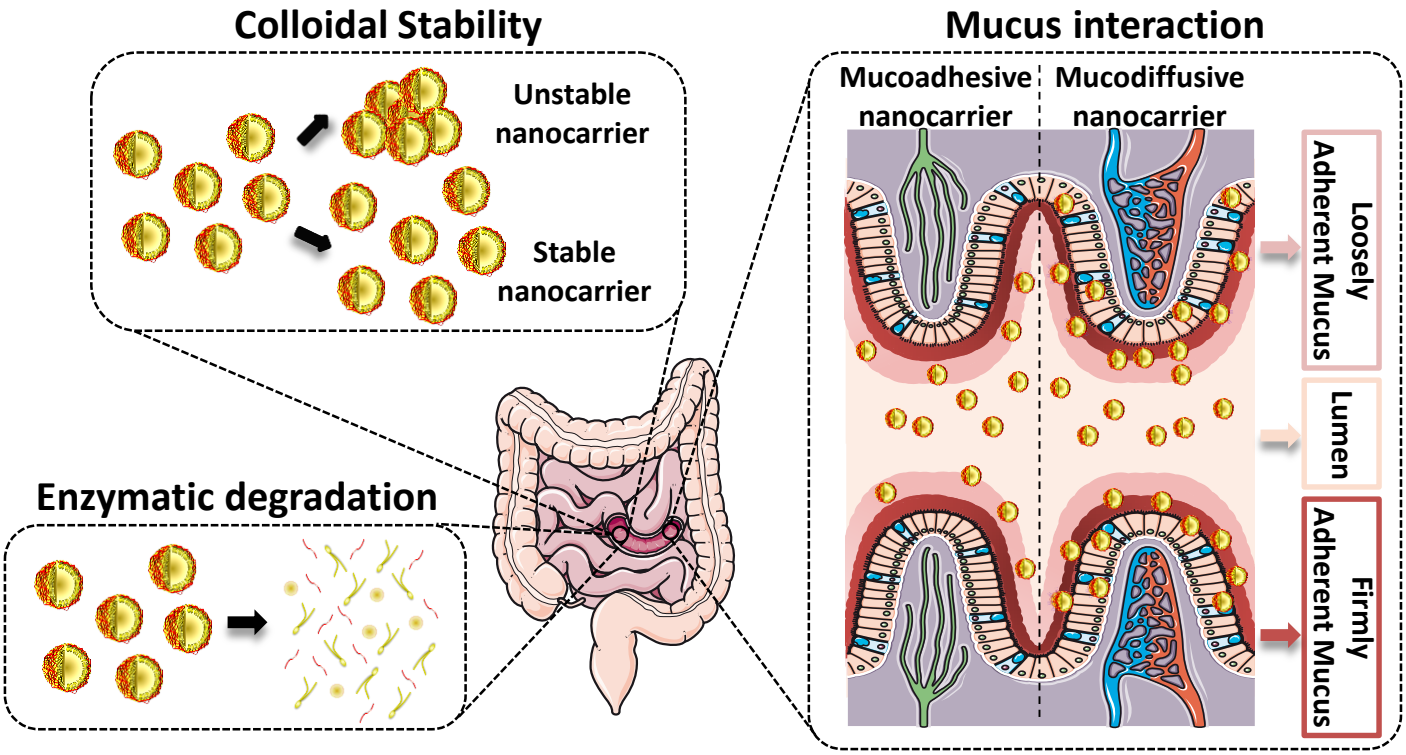

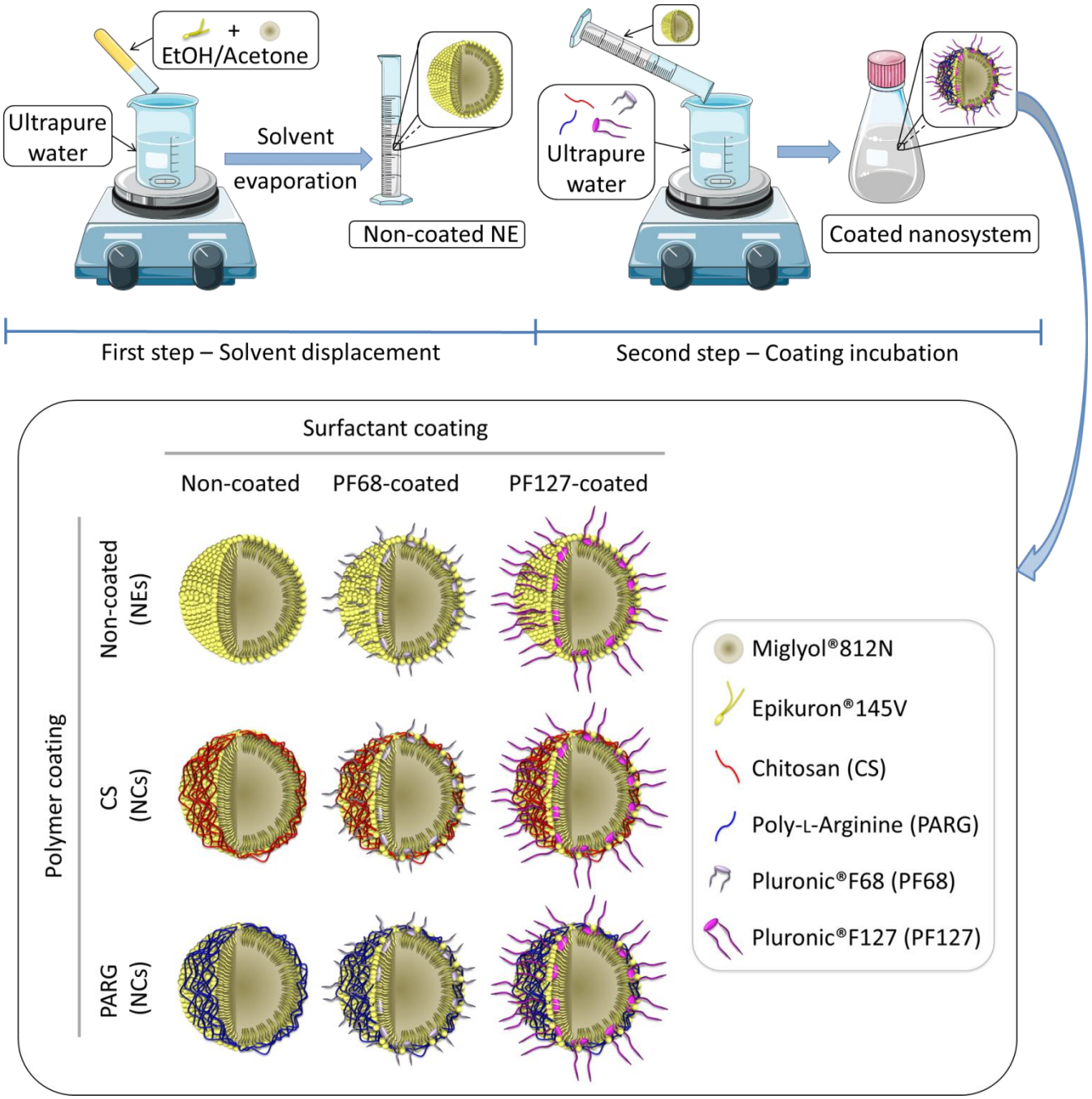

Figure 1. Schematic representation of the formulation procedure (upper panel) and the nanosystems tested (lower panel). Laboratory material and equipment (*https://creativecommons.org/licenses/by/3.0/*) have been modified from the original work provided by Servier Medical Art (*http://smart.servier.com/*).

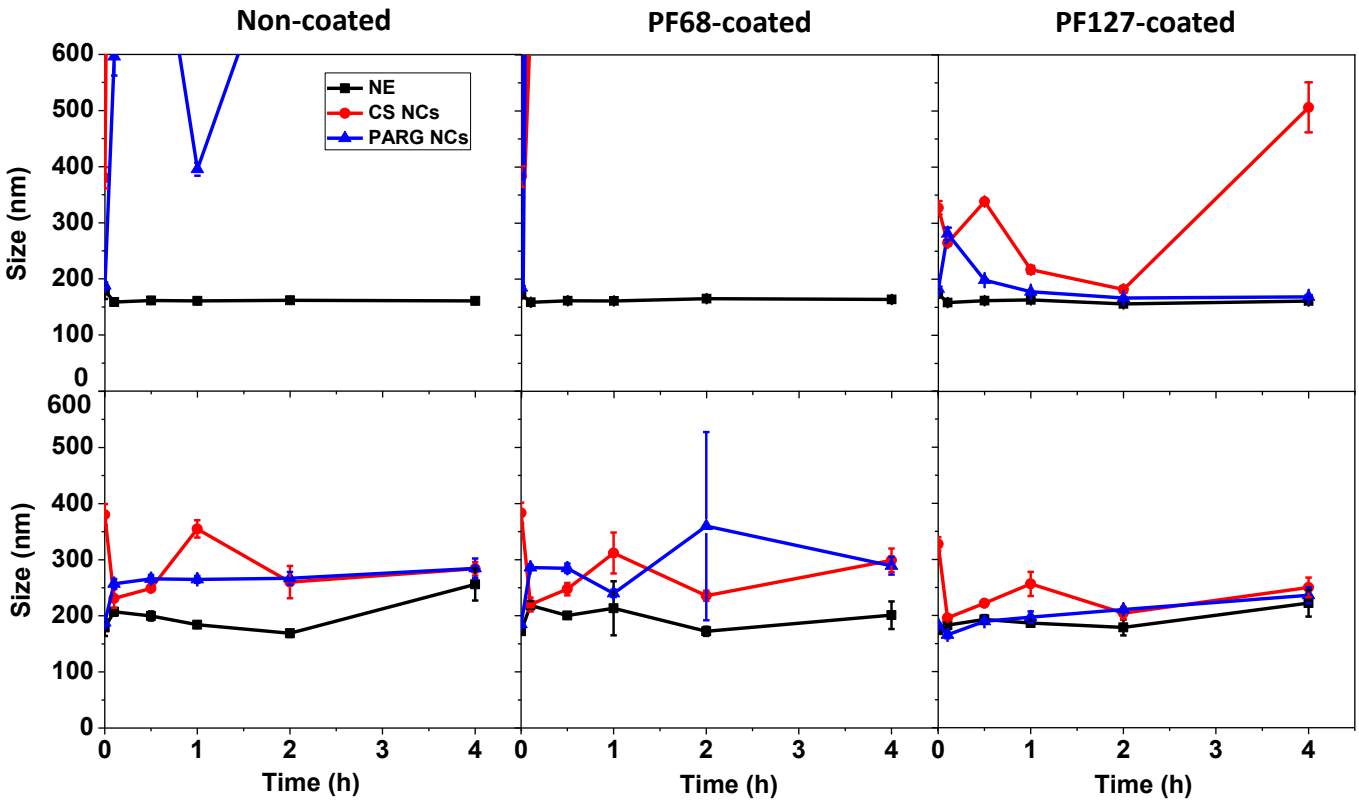

Figure 2. Colloidal stability in simulated intestinal fluid. *Hydrodynamic mean size of the NEs (black), CS NCs (red) and PARG NCs (blue) incubated either in SIF without enzymes (top) or in 1 % pancreatin supplemented SIF (bottom) (Error bars mean standard deviation; n ≥ 3).*

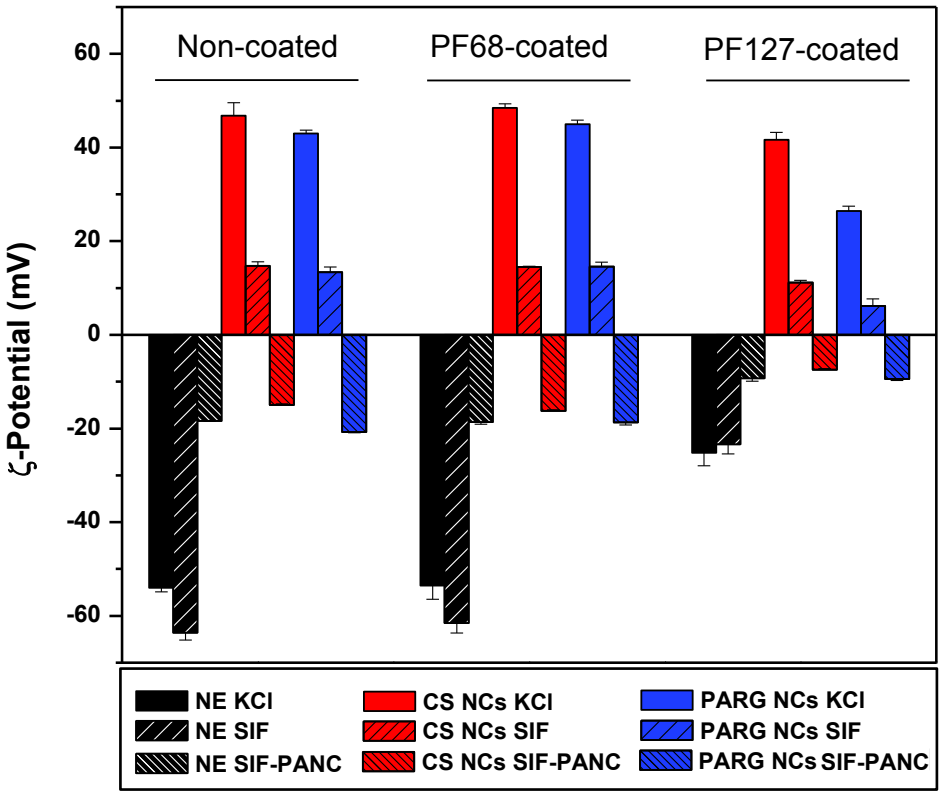

Figure 3. Surface charge of the nanosystem in different media. *ζ–potential (mV) of the NEs (black), CS NCs (red) and PARG NCs (blue) measured either in KCl 1 mM (closed bars), SIF without enzymes (sparse dashed bars) or 1 % pancreatin supplemented SIF (dashed bars) (Error bars mean standard deviation; n ≥ 3).*

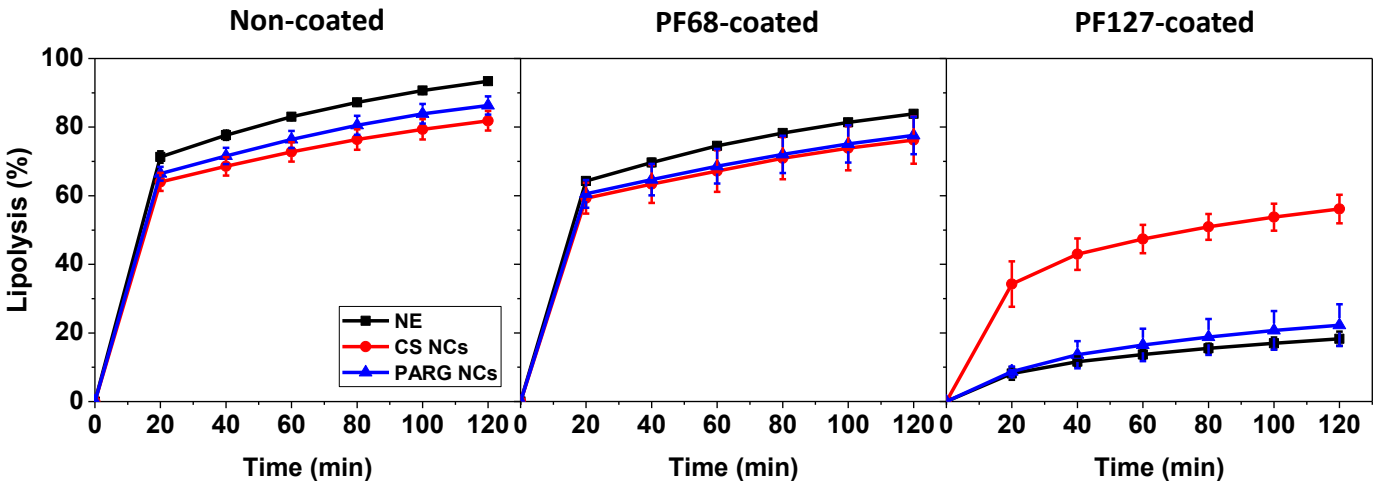

Figure 4. Lipolysis in simulated intestinal fluid. *Percentage of lipolysis of the NEs (black), CS NCs (red) and PARG NCs (blue) incubated in SIF. Degradation of the non-coated NE after 5 hours of incubation in SIF was set as 100 % of degradation (Error bars mean standard deviation; n ≥ 3).*

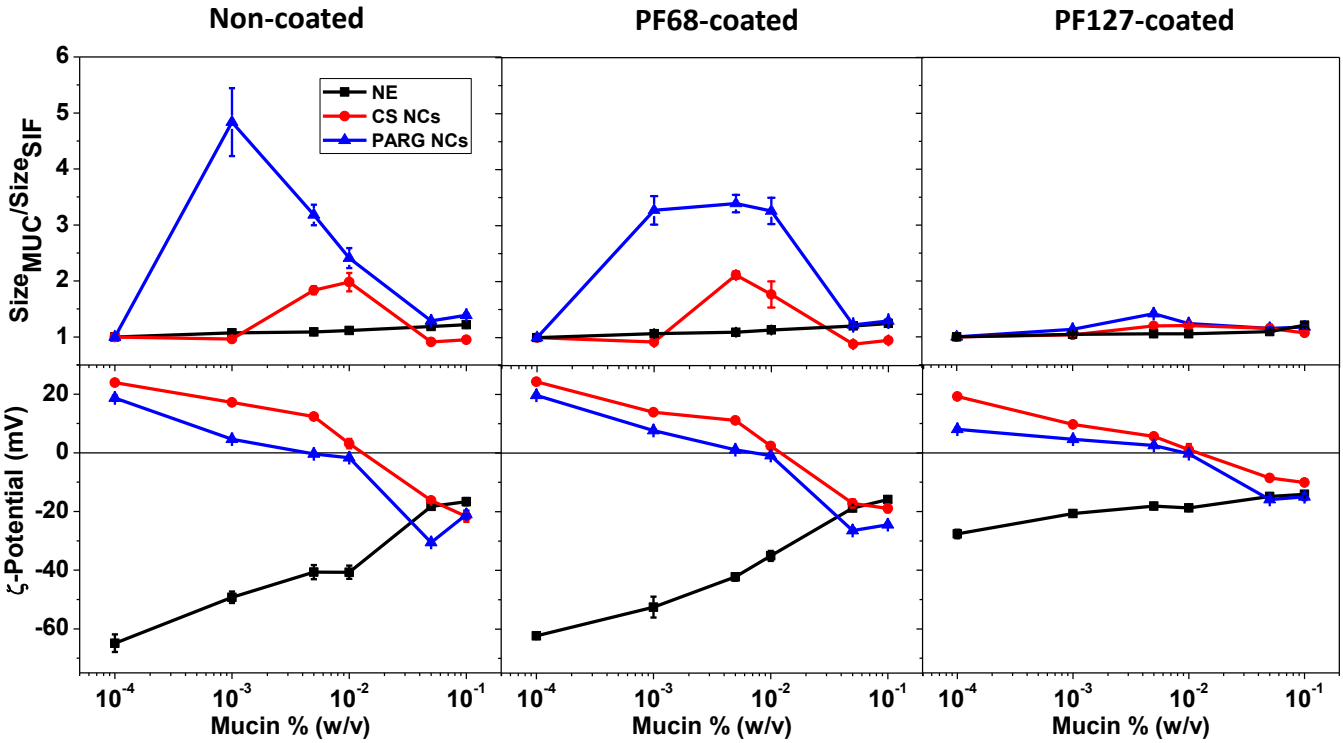

Figure 5. Mucoadhesion assessed by the dynamic light scattering approach. *Hydrodynamic mean size increase, expressed as $Size_{Mucin}/Size_{SIF}$ ratio (top), and ζ−potential modification (bottom) of the NEs (black), CS NCs (red) and PARG NCs (blue) incubated in mucin solutions in diluted SIF (1/25) without enzymes with a concentration ranging from 1 x 10^{-4} to 1 x 10^{-1} % (w/v) (Error bars mean standard deviation; n ≥ 3).*

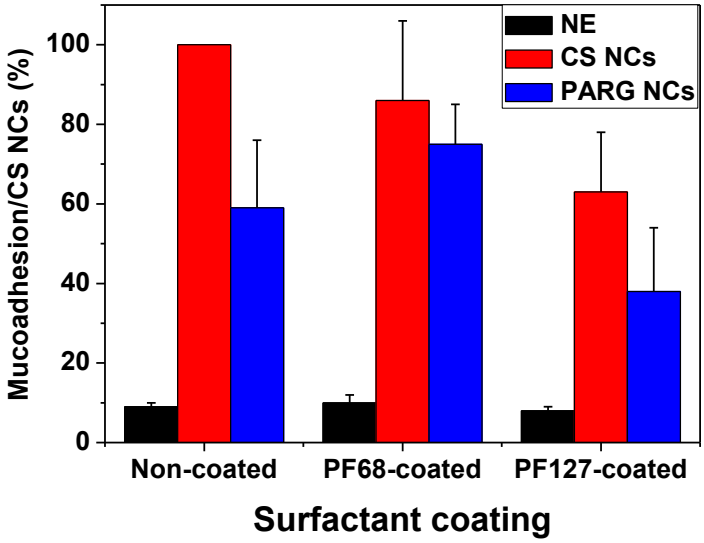

Figure 6. Mucoadhesion assessed by the fluorescence microscopy approach. *Adhesion percentage upon incubation with a mucin film of the NEs (black), CS NCs (red) and PARG NCs (blue) compared to the non-coated CS NCs (set as 100 %) (Error bars mean standard deviation; n ≥ 3).*

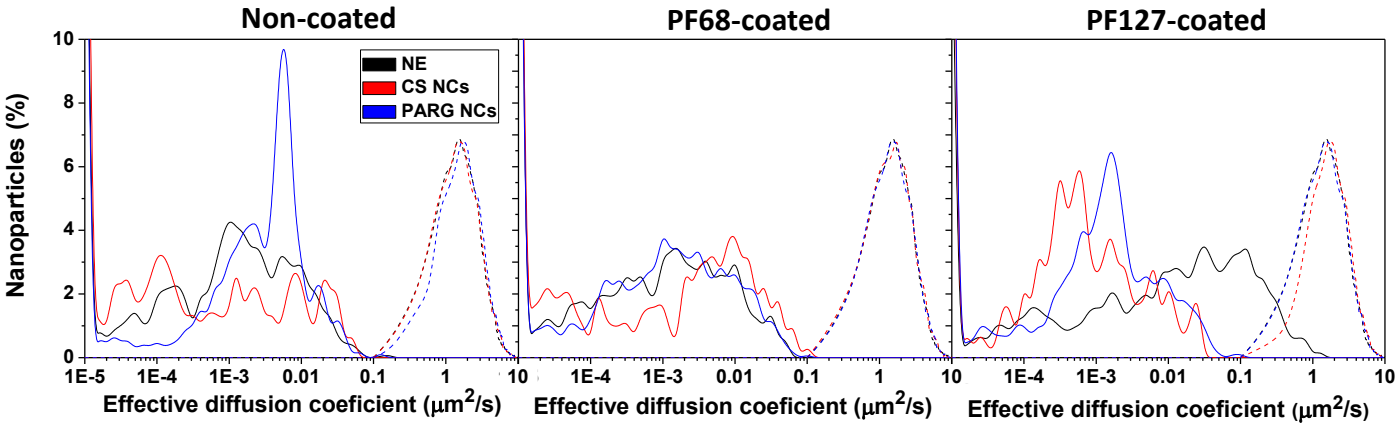

Figure 7. Mucodiffusion assessed by multiple particle tracking analysis. *Histogram of the effective diffusion coefficient (D_e) of the different nanosystems tested in intestinal porcine mucus (continuous line) and in PBS (dotted line) calculated at a time scale of 1 second. Non-coated (left), PF68-coated (middle) and PF127-coated (right) NEs (black), CS NCs (red) and PARG NCs (blue) (number of batches analyzed n = 3; n ≥ 1000 nanoparticles/oily droplets).*

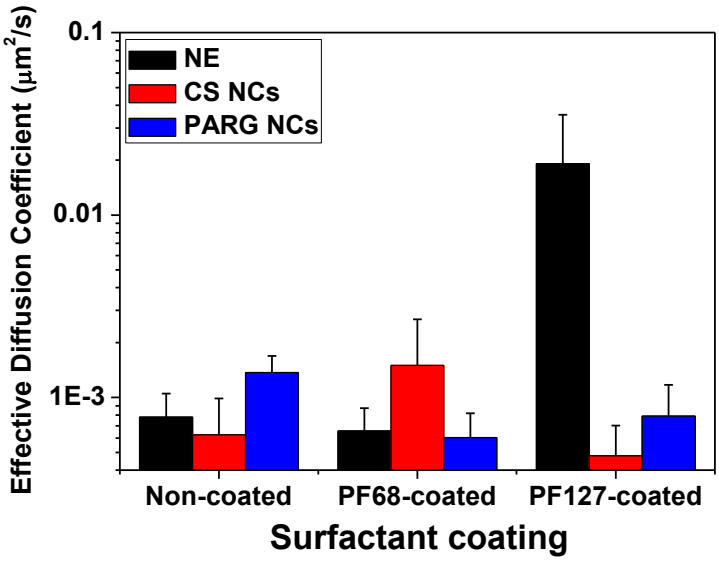

Figure 8. Mucodiffusion assessed by multiple particle tracking analysis. *Mean effective diffusion coefficient of the non-coated, PF68-coated, and PF127-coated NEs (black), CS NCs (red) and PARG NCs (blue) calculated from their trajectories in porcine intestinal mucus at 37 °C at a time scale of 1 second (Error bars mean standard deviation; number of batches analyzed n = 3; n ≥ 1000 nanoparticles/oily droplets).*

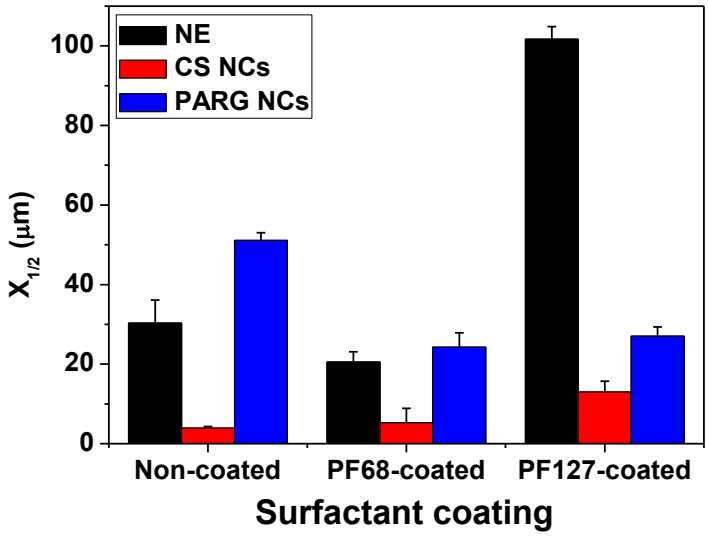

Figure 9. Mucodiffusion assessed by the capillary approach. *Mean penetration capacity ($X_{1/2}$) of the non-coated, PF68-coated and PF127-coated NEs (black), CS NCs (red) and PARG NCs (blue) according to their penetration profile through a capillary filled with porcine mucus at 37 °C (Error bars mean standard deviation; n ≥ 3).*